International Journal of Engineering Applied Sciences and Technology, 2023
Vol. 8, Issue 01, ISSN No. 2455-2143, Pages 383-392
Published Online May 2023 in IJEAST (http://www.ijeast.com)

DEVELOPMENT OF MODIFIED CONSTANT-FORCE COMPRESSION SLIDER MECHANISMS

Ikechukwu Celestine Ugwuoke
Department of Mechanical Engineering,
Federal University of Technology, Minna, Nigeria.

Abstract—**The original Constant-Force Compression Slider Mechanisms (CSMs) contain flexure hinges in the form of slender beams which degrades the performance of these CSMs at high values of required transverse stiffness. This work focused on the development of modified constant-force CSMs that will serve as a possible replacement for the original configurations possessing short-length flexural pivots in requiring higher values of transverse stiffness. This class of mechanisms also generate a constant output force over a wide range of slider input displacements. Based on the principle of Static Equivalence, a Generalized Mathematical Static Model (GMSM) was developed for all modified constant-force CSMs. Performance testing of the modified constant-force CSM shows a great improvement in transverse stiffness when compared with the original constant-force CSMs. Comparison between Class 1A-lppm and Class 1A-spp, between Class 1B-plpm and Class 1B-psp, between Class 2A-llpm and Class 2A-ssp, between Class 2B-lplm and Class 2B-sps, and between Class 3A-lllm and Class 3A-sss show an increase of 2291.90%, 2927.36%, 1007.08%, 2559.12%, and 443.97% respectively in the amount of constant-force. This class of modified constant-force CSMs is well-suited for applications requiring higher values of transverse stiffness.**

Keywords—**Modified Constant-force, Compression slider mechanisms, Great improvement, Transverse stiffness, Performance evaluation.**

I. INTRODUCTION

Compliant Mechanisms (CMs) are a class of mechanisms that utilize compliance of their constituent elements to transmit motion/or force. They are particularly suited for applications with a small range of motions [7]. Burns [2] undertook the first academic study to diverge from the popular underlying notion that links of a mechanism should be considered rigid. He and subsequent researchers recognized a number of advantages associated with this class of flexible mechanisms [1; 3; 8; 12; 13; 14;15; 16]. Traditionally, the large non-linear deflections have caused significant difficulties in the design of CMs. Techniques such as finite element analysis (FEA) and elliptic integrals provide accurate information but make the design very drawn out and complicated. Fortunately, the development of the PRBM has greatly increased the speed and ease with which CMs can be designed [4]. Constant-Force Compression Slider Mechanisms (CSMs) are mechanisms that generate a constant output force over a wide range of input displacements [12; 13]. The original CSMs as shown in Figure 1 contain short-length flexural pivots in the form of slender beams that attempt to mimic the hinges. Although these slender beams have low rotational stiffness, they have a deficiency in that they also possess a low axial stiffness when deflected from the straight configuration, and they possess a low buckling strength [16]. These slender beams degrade the performance of the original CSMs at higher values of required transverse stiffness [12; 16]. The principal focus of this research was to develop modified constant-force CSMs that will serve as a possible replacement for the original CSMs possessing short-length flexural pivots in applications requiring higher values of transverse stiffness.

II. DESCRIPTION OF THE MODIFIED CSMS

Using type-synthesis techniques, Murphy [1], and Murphy et al. [9], generated 28 possible constant-force CSMs. Howell et al. [5] carried out the dimensional synthesis of several of these CSMs. Fig. 1 shows the side-by-side comparison of the modified constant-force CSMs with the original constant-force CSMs. These mechanisms have been divided into 5 classifications based on the number of flexible segments and their location in each CSMs [12, 16]. As shown in Fig. 1, Class 1A mechanisms are CSMs that have one flexible segment located at the first pivot point, Class 1B CSMs have one flexible segment located at the second pivot point, Class 2A CSMs have two flexible segments located at the first and second pivot points, Class 2B CSMs have two flexible segments located at the first and third pivot points, Class 3A CSMs have three flexible segments located at the first, second, and third pivot points. Each of the CSMs shown in Fig. 1 is denoted by a string of letters representing the order and type of pivots used. The letters “s”, “l”, “p”, and “m” represents small-length flexural pivot, long flexible beam, pin joint, and modified respectively [12].

International Journal of Engineering Applied Sciences and Technology, 2023
Vol. 8, Issue 01, ISSN No. 2455-2143, Pages 383-392
Published Online May 2023 in IJEAST (http://www.ijeast.com)

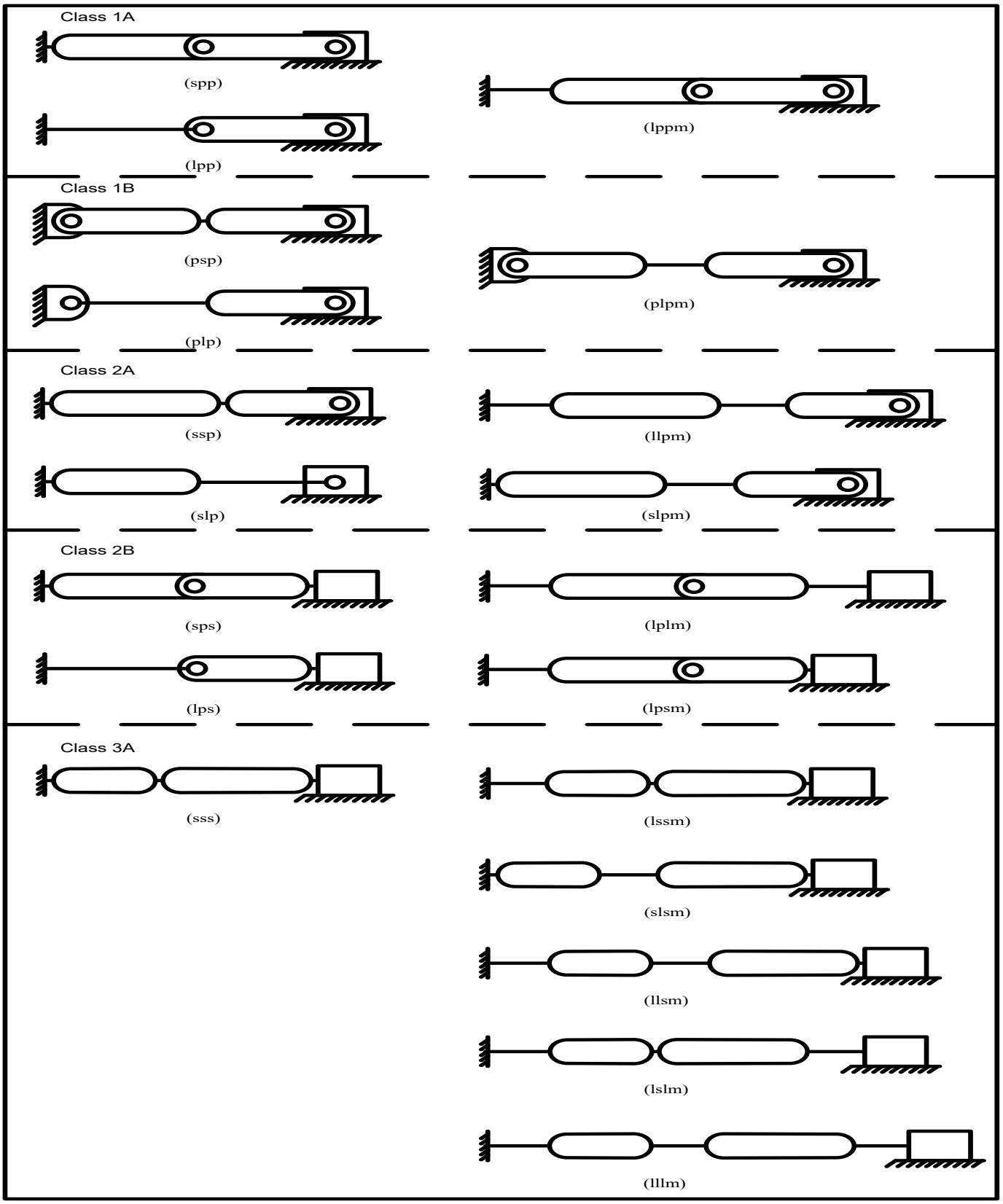

Fig. 1: Side-by-side comparison of the modified CSMs with the original CSMs [12]

International Journal of Engineering Applied Sciences and Technology, 2023
Vol. 8, Issue 01, ISSN No. 2455-2143, Pages 383-392
Published Online May 2023 in IJEAST (http://www.ijeast.com)

III. THE GENERALIZED PSEUDO-RIGID-BODY MODEL (PRBM)

The generalized PRBM for all the modified CSMs presented in Fig. 1 is shown in Fig. 2; only half of the symmetric mechanism is shown. Each of the modified CSMs presented in Fig. 1 can be converted to its equivalent rigid-body counterpart by using the PRBM rule for small-length flexural pivots, the PRBM rule for modified long fixed-pinned flexible beams, the PRBM rule for modified long fixed-fixed flexible beams, or a combination of the PRBM rules [12]. The most straightforward alteration is that every flexible segment becomes two rigid segments joined by a pin and torsional spring [1; 6; 12; 13; 14;15; 16].

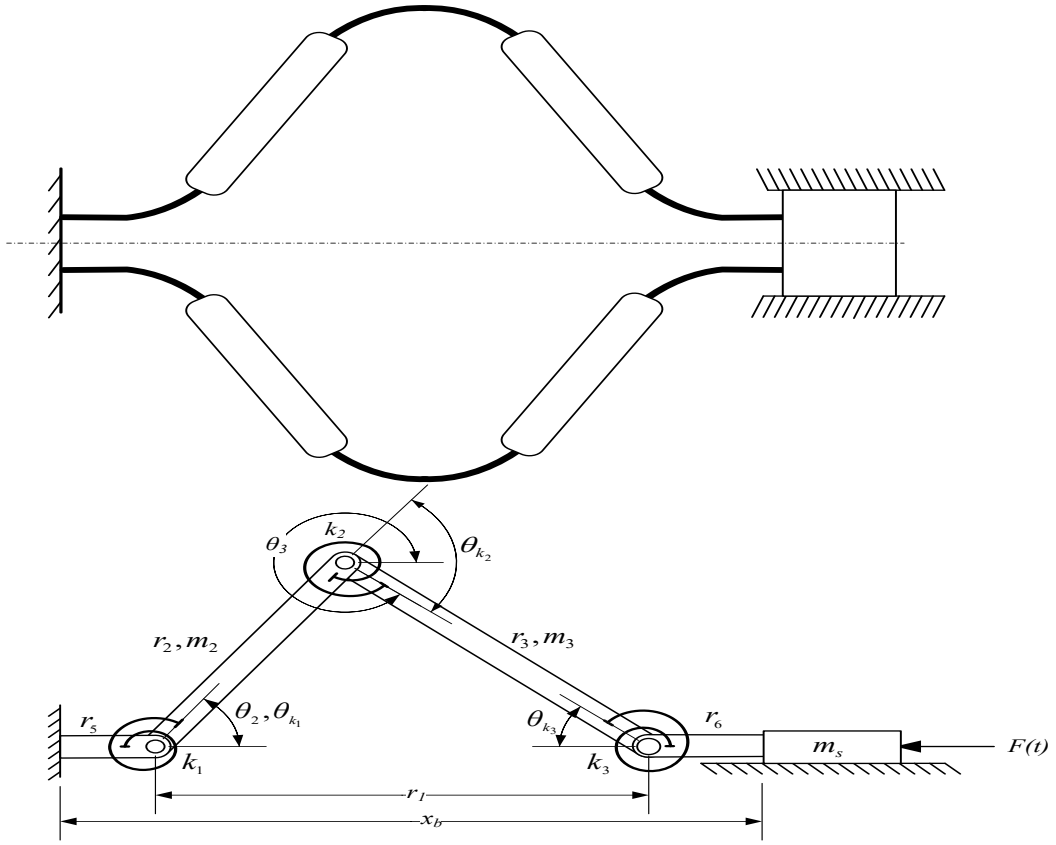

Fig. 2: Modified Constant-Force CSM Class 3A-lllm, and the Generalized PRBM [12; 13]

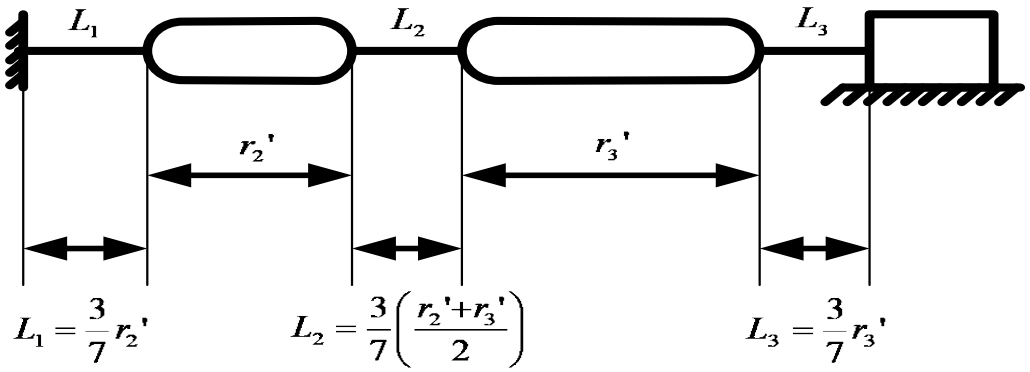

Fig. 3. Definition of flexible and rigid segment lengths

International Journal of Engineering Applied Sciences and Technology, 2023
Vol. 8, Issue 01, ISSN No. 2455-2143, Pages 383-392
Published Online May 2023 in IJEAST (http://www.ijeast.com)

Table 1. Mechanisms combination that formed the modified constant-force CSMs [12]

Modified CSMs	Combined CSMs
Class 1A-lppm	Class 1A-spp, Class 1A-lpp
Class 1B-plpm	Class 1B-psp, Class 1B-plp, Class 1B-plpFle
Class 2A-llpm	Class 2A-ssp, Class 2A-slp, Class 2A-llpFle, Class 2A-llpRig
Class 2B-lplm	Class 2B-sps, Class 2B-lps, Class 2B-lplFle, Class 2B=lplRig
Class 3A-lllm	Class 3A-sss, Class 3A-llsRig, Class 3A-lllFle, Class 3A-lllRig

Table 2. Flexible and rigid segment lengths for the modified constant-force CSMs [12]

To get:	L_1	L_2	L_3	r_2'	r_3'
Modified CSMs	Multiply r_2 by	Multiply r_{ave}' by	Multiply r_3' by	Subtract from r_2	Subtract from r_3
Class 1A-lppm	3/7	0	0	$0.5\times L_1$	0
Class 1B-plpm	0	3/7	0	$0.5\times L_2$	$0.5\times L_2$
Class 2A-llpm	3/7	3/7	0	$0.5\times(L_1+L_2)$	$0.5\times L_2$
Class 2B-lplm	3/7	0	3/7	$0.5\times L_1$	$0.5\times L_3$
Class 3A-lllm	3/7	3/7	3/7	$0.5\times(L_1+L_2)$	$0.5\times(L_2+L_3)$

Table 1 shows the CSMs combination that formed each of the modified CSMs that was investigated. Table 2 gives the flexible and rigid segment lengths for the modified CSMs. The definition in Fig. 3, together with those tabulated in Table 3, may be used to determine the length of the flexible and rigid segments for all modified CSMs investigated [15]. Using Lagrange's method of formulation, taking θ_2 as the generalized position coordinate, and neglecting the effect of damping on the modified CSM model, Lagrange's equation for a static system may be expressed as [11;12; 13; 14]

$$\frac{\delta(V)}{\delta\theta_2} = Q_{\theta 2} \quad (1)$$

The generalized forcing function $Q_{\theta 2}$ consists of a moment τ_F due directly to the force Facting on the sliderand the terms τ_{CF} and τ_{AF} are introduced to compensate for the moment due to Coulomb pin friction and that due to axial force effects in the mechanism's pin joints, and links/segments of the modified CSMs respectively [1; 12].In mathematical terms, the generalized forcing function $Q_{\theta 2}$ is given by the following expression

$$Q_{\theta 2} = \frac{\delta(V)}{\delta\theta_2} = \tau_F + \tau_{CF} + \tau_{AF} \quad (2)$$

The total potential energy in the mechanism assuming negligible potential energy due to gravity is the sum of the individual potential energy stored in each compliant segment. For the modified CSM model, the generalized potential energy equation is given as [1, 12, and 16]

$$V = \frac{1}{2}(k_1\theta_{k1}^2 + k_2\theta_{k2}^2 + k_3\theta_{k3}^2) \quad (3)$$

Wherek_1,k_2, and k_3 are the torsional spring constants andθ_{k1}, θ_{k2}, and θ_{k3} are the relative deflections of the torsional springs which may be obtained from the following expressions [1; 12; S16]

$$\theta_{k1} = \theta_2 \quad (4)$$

$$\theta_{k2} = \theta_2 + \theta_{k3} \quad (5)$$

$$\theta_{k3} = \sin^{-1}\left(\frac{r_2}{r_3}\sin\theta_2\right) \quad (6)$$

Substituting equations (4), (5), and (6) into equation (3), the expression for the potential energy therefore becomes

$$V = \frac{1}{2}\left(k_1\theta_2^2 + k_2\left(\theta_2 + \sin^{-1}\left(\frac{r_2}{r_3}\sin\theta_2\right)\right)^2 + k_3\left(\sin^{-1}\left(\frac{r_2}{r_3}\sin\theta_2\right)\right)^2\right) \quad (7)$$

The generalized expression for the moment due to Coulomb pin friction τ_{CF} is given as [12]

$$\tau_{CF} = \left(C_1\theta_2 + C_2\theta_2\left(1 + \frac{r_2\cos\theta_2}{\sqrt{r_3^2 - r_2^2\sin^2\theta_2}}\right) + C_3\theta_2\left(\frac{r_2\cos\theta_2}{\sqrt{r_3^2 - r_2^2\sin^2\theta_2}}\right)\right)\text{sign}\left(\dot{\theta_2}\right) \quad (8)$$

Where C_1, C_2, and C_3 are the coulomb friction coefficients at the different pivot points, usually obtained from the experiment. The value of the torque τ_{AF} may be approximated using the following expression [12]

International Journal of Engineering Applied Sciences and Technology, 2023
Vol. 8, Issue 01, ISSN No. 2455-2143, Pages 383-392
Published Online May 2023 in IJEAST (http://www.ijeast.com)

$\tau_{AF} = F_{static} r_2 \alpha \left(1 + \frac{r_2}{\sqrt{r_3^2 - r_2^2\alpha^2}}\right) \propto$is the angle of axial force effect (9)

Substituting equations (7), (8), and (9) into equation (2) and simplifying, the Generalized Mathematical Static Model (GMSM) for allmodified constant-force CSMs is obtained as [12]

$$F = \left[\frac{1}{\left(-r_2\sin\theta_2 - \frac{r_2^2\sin\theta_2\cos\theta_2}{\sqrt{r_3^2 - r_2^2\sin^2\theta_2}}\right)}\right] \times \left[k_1\theta_2 + k_2\left(\theta_2 + \sin^{-1}\left(\frac{r_2}{r_3}\sin\theta_2\right)\right)\left(1 + \frac{r_2\cos\theta_2}{\sqrt{r_3^2 - r_2^2\sin^2\theta_2}}\right) + k_3\left(\sin^{-1}\left(\frac{r_2^2\sin\theta_2\cos\theta_2}{\sqrt{r_3^2 - r_2^2\sin^2\theta_2}}\right)\right)\left(\frac{r_2\cos\theta_2}{\sqrt{r_3^2 - r_2^2\sin^2\theta_2}}\right) - \left(C_1\theta_2 + C_2\theta_2\left(\frac{r_2\cos\theta_2}{\sqrt{r_3^2 - r_2^2\sin^2\theta_2}}\right) + C_3\theta_2\left(\frac{r_2\cos\theta_2}{\sqrt{r_3^2 - r_2^2\sin^2\theta_2}}\right)\right)\text{sign}\dot{\theta_2} - F_{static} r_2 \alpha\left(1 + \frac{r_2}{\sqrt{r_3^2 - r_2^2\alpha^2}}\right)\right] \quad (10)$$

IV. EXPERIMENTATION AND DISCUSSION OF RESULTS

Table 3 gives the parameters and values for the modified constant-force CSMs investigated. Table 4 gives the mechanism's extended length, fully compressed length, nominal constant force, and average non-dimensionalized constant for a 40% slider displacement. The accuracy of the modified CSM model was verified by comparing the predicted results with the test results as demonstrated in Fig. 5 through 9. Three interesting phenomena were observed in every test carried out. First, since there was no pre-displacement on the modified CSM, the initial force must be zero. However, as the modified CSM goes through the initial displacement, there was a sharp rise from zero force to the intended constant force. This phenomenon was also observed by Millar et al. [8] during the initial testing of CSMs. The phenomenon was easily addressed by giving the modified CSM a 10% pre-displacement. The second phenomenon observed was that the average output force for both compression and expansion of the modified constant-force CSMs was below that predicted by the Modified CSM model. The same phenomenon was also observed by Evans and Howell [3] during the testing of the robotic arm end-effector coupling device. This phenomenon was attributed to the minor flexibility of the portion of the modified constant-force CSMs that was assumed to be rigid [12]. The third phenomenon observed was that there was a difference in force between the expansion and compression strokes of the test. During the compression stroke, the modified CSMs experienced a higher force which was greater than that predicted by the modified CSM model. As the mechanism reverses direction, there was a sharp decrease in the force which was lower than that predicted by the modified CSM model. This phenomenon was attributed to friction within the pin joints of the modified constant-force CSMs and the testing equipment, which acted to oppose the motion of the modified CSMs [12]. While the modified CSM was being compressed, the frictional forces opposed the direction of the output force, and vice versa when the device was allowed to expand. This friction caused the actual output force of the modified CSM to deviate from the predicted output force by an amount proportional to the level of friction. This frictional effect can be removed by averaging the measured data obtained during both the compression and expansion strokes. This same phenomenon was also observed by Boyle [1], Evans and Howell [3], Millar et al. [8], Ugwuoke [12], and Weight [16].

International Journal of Engineering Applied Sciences and Technology, 2023
Vol. 8, Issue 01, ISSN No. 2455-2143, Pages 383-392
Published Online May 2023 in IJEAST (http://www.ijeast.com)

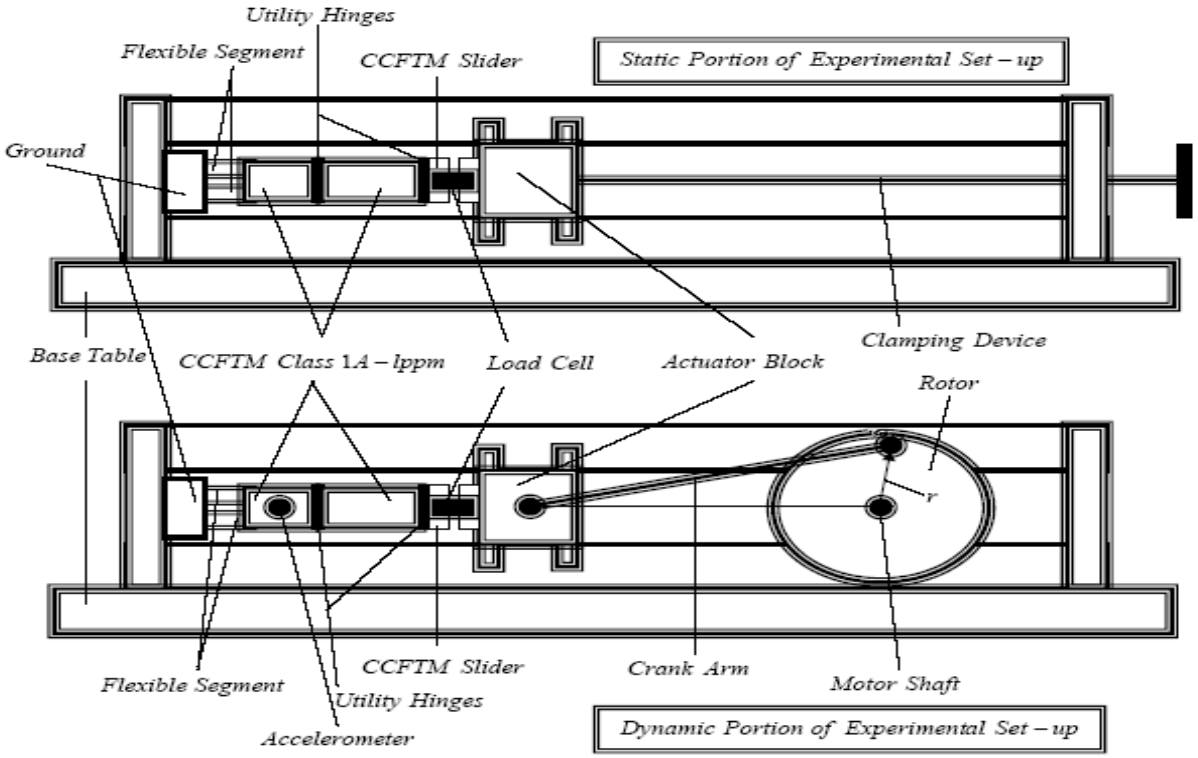

Fig. 4. Schematic of the Multi-purpose Experimental Set-up [12]

The results obtained for the modified constant-force CSMs investigated show that they possess highly improved transverse stiffness capabilities. Table 5 shows the summary of the simulation results comparison between the modified CSMs and the original CSMs which incorporates short-length flexural pivots. As shown in Table 5, a comparison between Class 1A-lppm and Class 1A-spp, between Class 1B-plpm and Class 1B-psp, between Class 2A-llpm and Class 2A-ssp, between Class 2B-lplm and Class 2B-sps, and between Class 3A-lllm and Class 3A-sss show an increase of 2291.90%, 2927.36%, 1007.08%, 2559.12%, and 443.97% respectively in the amount of constant-force. Figure 4 shows the schematic of the multi-purpose experimental setup that was used to validate the static model. The experimental setup shown in Figure 4 can also be used for the dynamic testing of CSMs [12]. A static test was performed by transferring the modified CSM to the static part of the experimental setup and giving the modified CSM a pre-displacement using a clamping device. The clamp is slowly screwed tight compressing the modified CSM, and then unscrewed allowing the modified CSM to expand back to its initial position. Bolted in-line between the clamping device and the modified CSM is a load cell that measures the force exerted on the slider. The load cell used is a Compression Digital USB Load Cell with digital perfection for load and force measurement (UP-C-050-005), with a load capacity of 222.4N and an accuracy of 0.050%. It offers direct measurement of loads via the USB port of a PC, it does not require signal conditioners, data acquisition systems, or special software. The power supply is via a USB port with integrated power conditioning. It is mechanically robust, rugged, and has a compact design with a low profile and stainless steel construction. It also has a threaded mounting hole for easy attachment using standard fixtures. A linear potentiometer measures the slider displacement. Table 6 gives the summary of the comparisons of the results between that obtained from the test and that predicted by the CSM model.

Table 3. Parameters and Values for the modified constant-force CSMs

Modified CSM Class	1A-lppm	1B-plpm	2A-llpm	2B-lplm	3A-lllm
r_2	73.5135 mm	84.2105 mm	71.3580 mm	68.0000 mm	69.5652 mm
r_3	73.5135 mm	75.7895 mm	78.4938 mm	68.0000 mm	69.5652 mm
r_5	12.9730 mm	-	10.4215 mm	12.0000 mm	10.4348 mm
r_6	-	-	-	12.0000 mm	10.4348 mm
m_2	76.1446 g	78.3494 g	97.1555 g	74.1147 g	96.4089 g

International Journal of Engineering Applied Sciences and Technology, 2023
Vol. 8, Issue 01, ISSN No. 2455-2143, Pages 383-392
Published Online May 2023 in IJEAST (http://www.ijeast.com)

m_3	51.8910 g	75.3607 g	76.5531 g	74.1147 g	96.4089 g
m_s	151.5958 g	151.5958 g	151.5958 g	233.4276 g	233.4276 g
b	25.40 mm	25.40 mm	25.40 mm	25.40 mm	25.40 mm
h_1	0.5602 mm	-	0.2102 mm	0.5181 mm	0.2253 mm
h_2	-	0.3042 mm	0.2652 mm	-	0.1126 mm
h_3	-	-	-	0.5181 mm	0.2253 mm
E	207 Gpa	207 Gpa	207 Gpa	207 Gpa	207 Gpa
l_1	25.9459 mm	-	20.8431 mm	24.0000 mm	20.8696 mm
l_2	-	28.2353 mm	24.6054 mm	-	20.8696 mm
l_3	-	-	-	24.0000 mm	20.8696 mm
k_1	4.0113 Nm	-	0.5279 Nm	3.4322 Nm	0.6488 Nm
k_2	-	0.5903 Nm	0.4487 Nm	-	0.0811 Nm
k_3	-	-	-	3.4322 Nm	0.6488 Nm
Mean Force	59.0781 N	32.0878 N	35.9813 N	109.2944 N	25.2446 N

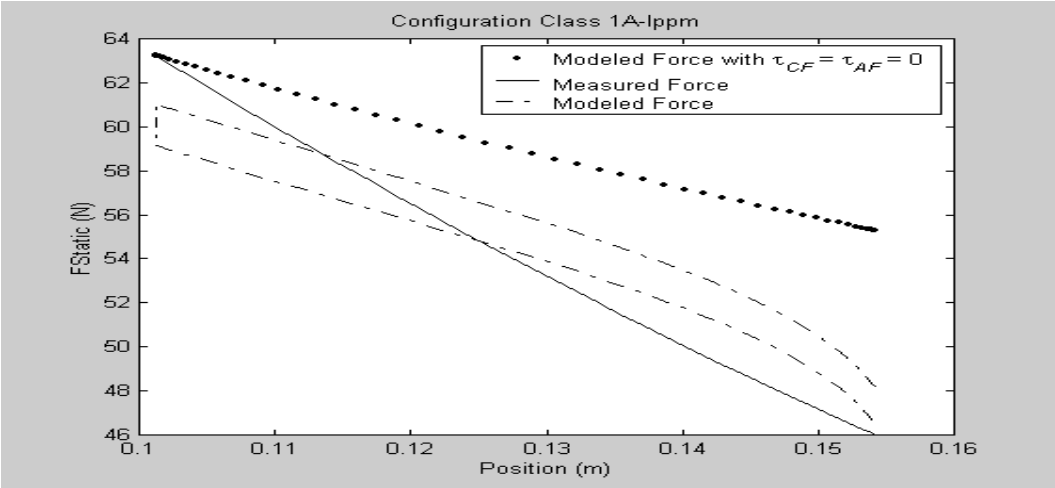

Fig. 5. Position-Force Diagram for Compression and Expansion of Modified CSM Class 1A-lppm

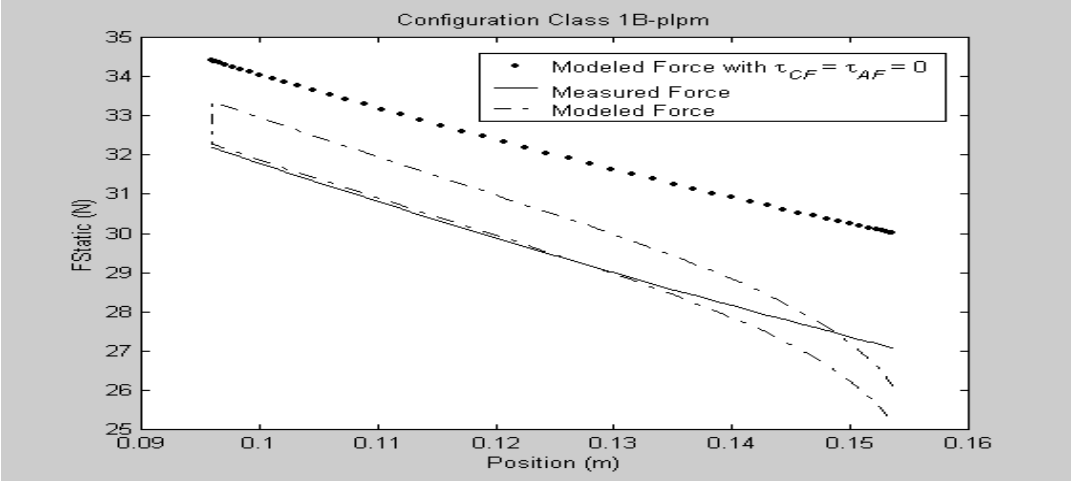

Fig. 6. Position-Force Diagram for Compression and Expansion of Modified CSM Class 1B-plpm

International Journal of Engineering Applied Sciences and Technology, 2023
Vol. 8, Issue 01, ISSN No. 2455-2143, Pages 383-392
Published Online May 2023 in IJEAST (http://www.ijeast.com)

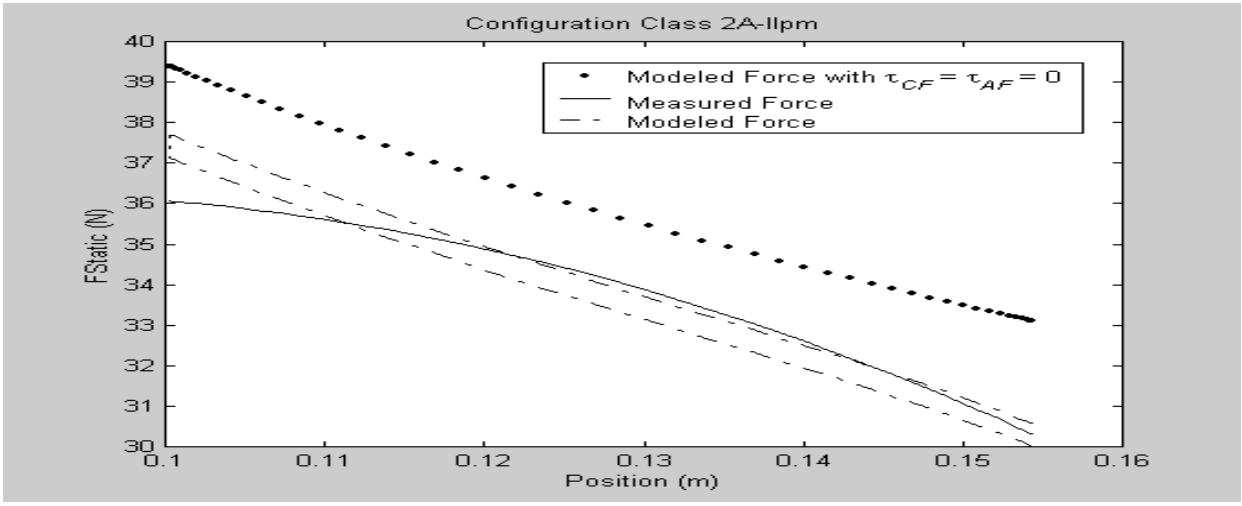

Fig. 7. Position-Force Diagram for Compression and Expansion of Modified CSM Class 2A-llpm

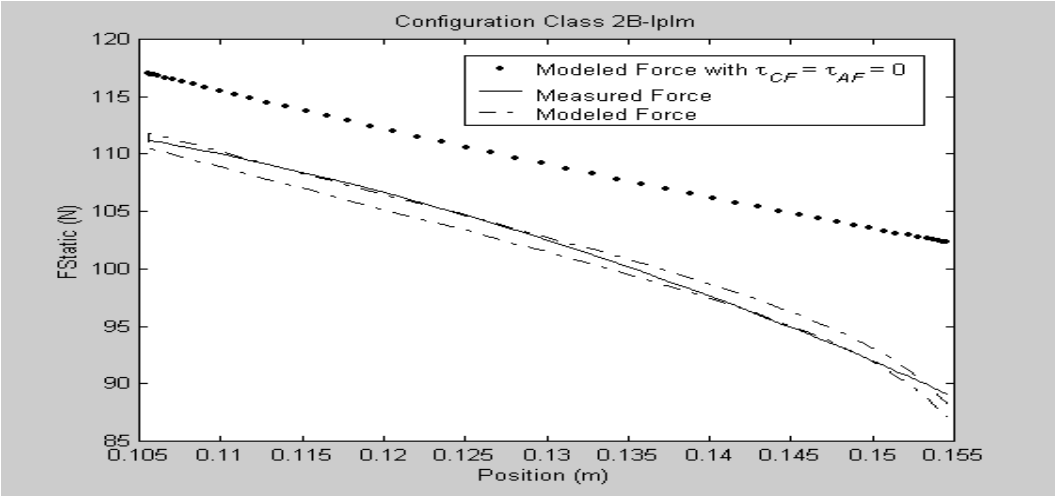

Fig. 8. Position-Force Diagram for Compression and Expansion of Modified CSM Class 2B-lplm

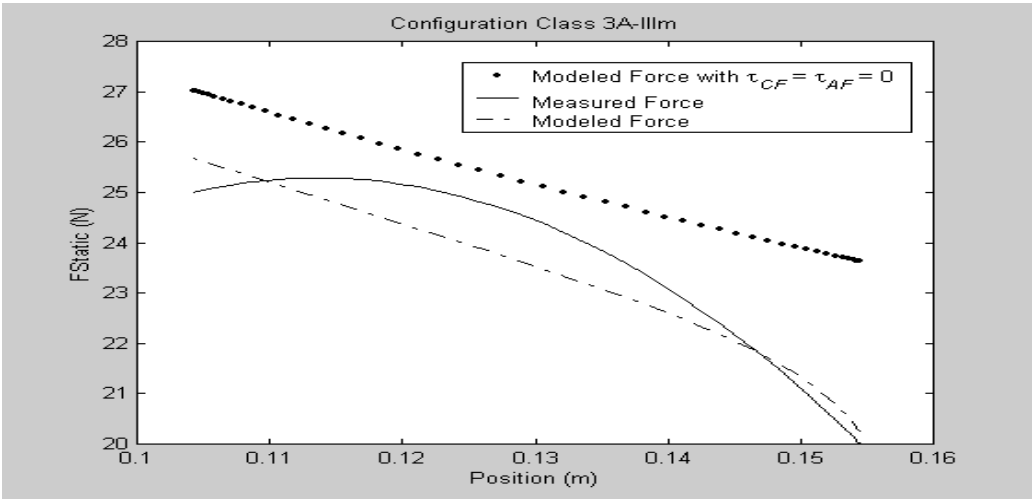

Fig. 9. Position-Force Diagram for Compression and Expansion of Modified CSM Class 3A-lllm

International Journal of Engineering Applied Sciences and Technology, 2023
Vol. 8, Issue 01, ISSN No. 2455-2143, Pages 383-392
Published Online May 2023 in IJEAST (http://www.ijeast.com)

Table 4. Extended length, fully compressed length, nominal constant-force, and average non-dimensionalized constant for a 40% displacement of the modified constant-force CSMs

Modified CSM Class	1A-lppm	1B-plpm	2A-llpm	2B-lplm	3A-lllm
x_b max	160.00 mm	160.00 mm	160.00 mm	160.00 mm	160.00 mm
x_b min	101.19 mm	96.00 mm	100.33 mm	105.60 mm	104.35 mm
F_{Nom}	59.08 N	32.09 N	34.82 N	109.29 N	25.24 N
ϕ	0.5413	2.2889	2.3533	1.0827	1.3534

Table 5. Summary of results comparison between the modified constant-force CSMs and the original constant-force CSMs incorporating small-length flexural pivots

Modified CSMs	Average Force (N)	Original CSMs	Average Force (N)	Percent Increase in Force (%)
Class 1A-lppm	59.08	Class 1A-spp	2.47	2291.90
Class 1B-plpm	32.09	Class 1B-psp	1.06	2927.36
Class 2A-llpm	35.98	Class 2A-ssp	3.25	1007.08
Class 2B-lplm	109.29	Class 2B-sps	4.11	2559.12
Class 3A-lllm	25.24	Class 3A-sss	4.64	443.97

Table 6. Summary of results comparison between measured and modeled force for the modified constant-force CSMs tested

Modified CSMs	Mean Force Test (N)	Mean Force Model (N)	Error (%)	Accuracy (%)
Class 1A-lppm	58.4468	58.5559	0.1091	99.8133
Class 1B-plpm	35.9368	36.0276	0.0908	99.7473
Class 2A-llpm	35.8402	35.9363	0.0961	99.7319
Class 2B-lplm	106.7106	106.7940	0.0834	99.9218
Class 3A-lllm	25.7502	25.6986	0.0516	99.7996

V. CONCLUSION

The original constant-force CSMs contain flexure hinges in the form of slender beams that attempt to mimic the local hinges. These slender beams degrade the performance of the original constant-force CSMs at high values of required transverse stiffness. This research focused on the development of modified constant-force CSMs that will serve as a possible replacement for the original configurations possessing short-length flexural pivots in applications requiring higher values of transverse stiffness. Based on the principle of Static Equivalence, a Generalized Mathematical Static Model (GMSM) was developed for all modified constant-force CSMs.Performance testing of the modified constant-force CSMs shows they possess highly improvedtransverse stiffness capabilities compared to the original constant-force CSMs containing short-length flexural pivots. Comparison between Class 1A-lppm and Class 1A-spp, between Class 1B-plpm and Class 1B-psp, between Class 2A-llpm and Class 2A-ssp, between Class 2B-lplm and Class 2B-sps, and between Class 3A-lllm and Class 3A-sss show an increase of 2291.90%, 2927.36%, 1007.08%, 2559.12%, and 443.97% respectively in the amount of constant-force. Three interesting phenomena were also observed in every test that was carried out. The first phenomenon observed was that since there was no pre-load on the modified constant-force CSM, the initial force must be zero. However, as the CSM goes through the initial displacement, there was a sharp rise from zero force to the intended constant force. The phenomenon was addressed by giving the modified CSM a 10% pre-displacement.The second phenomenon observed was that the average output force for both compression and expansion of the modified CSM was below that predicted by the model. This phenomenon was attributed to the minor flexibility of the portion of the modified CSM that was assumed to be rigid. The third phenomenon observed was that there was a difference in force between the expansion and compression strokes of the test. During the compression stroke, the modified CSM experienced a higher force which was greater than that predicted by the modified CSM model. As the mechanism reverses direction, there was a sharp decrease in the force which was lower than that predicted by the CSM model. This

phenomenon was attributed to friction within the pin joints of the modified constant-force CSM and the testing system, which acted to oppose the motion of the modified CSM. While the modified CSM was being compressed, the frictional forces opposed the direction of the output force, and vice versa when the device was allowed to expand. This friction caused the actual output force of the modified constant-force CSM to deviate from the predicted output force by an amount proportional to the level of friction. This frictional effect can be removed by averaging the measured data obtained during both the compression and expansion strokes.

VI. REFERENCE

[1] Boyle, C. L., 2001, "A Closed-Form Dynamic Model of the Compliant Constant-Force Mechanism using the Pseudo-Rigid-Body Model", M.S. Thesis, Brigham Young University, Provo, Utah.

[2] Burns, R. H., 1964, "The Kinetostatic Synthesis of Flexible Link Mechanisms", Ph.D. Dissertation, Yale University, New Haven, Connecticut.

[3] Evans, M. S. and Howell, L. L., 1999, "Constant-Force End-Effector Mechanism", Proceedings of the IASTED International Conference, Robotics and Applications, Oct. 28-30, Santa Barbara, CA, USA, pp. 250-256.

[4] Howell, L. L., 2001, "Compliant Mechanisms", John Wiley and Sons, New York.

[5] Howell, L. L., Midha, A., and Murphy, M.D, 1994, "Dimensional Synthesis of Compliant Constant-Force Slider Mechanisms", Machine Elements and Machine Dynamics, DE, Vol. 71, pp. 509-515.

[6] Howell, L. L. and Midha, A., 1995, "Parametric Deflection Approximations for End-Loaded Large Deflection Beams in Compliant Mechanisms", ASME Journal of Mechanical Design, Vol. 117, No. 1, pp. 156-165.

[7] Kota, S., Hetrick, J., Li, Z., and Saggere, L., 1999, "Tailoring Unconventional Actuators Using Compliant Transmissions: Design Methods and Applications", IEEE/ASME Transactions on Mechatronics, Vol. 4, No. 4, December 1999, pp. 396-408.

[8] Millar, A. J., Howell, L. L., and Leonard, J. N., 1996, "Design and Evaluation of Compliant Constant-Force Mechanisms", Proceedings of the 1996 ASME Design Engineering Technical Conferences and Computers in Engineering Conference, 96-DETC/MECH-1209.

[9] Murphy, M. D., Midha, A., and Howell, L. L., 1994, "Methodology for the Design of Compliant Mechanisms Employing Type Synthesis Techniques with Example", Proceedings of the 1994 ASME Mechanisms Conference, DE, Vol. 70, pp. 61-66.

[10] Murphy, M. D., 1993, "A Generalized Theory for the Type Synthesis and Design of Compliant Mechanisms", Ph.D Dissertation, Purdue University, West Lafayette, Indiana.

[11] Sandor, G. N. and Erdman, A. G., 1988, "Advanced Mechanism Design: Analysis and Synthesis", Volume 2, Prentice-Hall, New Delhi, pp. 435-530.

[12] Ugwuoke, I. C., 2010, Dynamic Modeling and Simulation of Compliant Constant-Force Mechanisms, Ph.D Thesis, Department of Mechanical Engineering, Federal University of Technology, Minna, Nigeria.

[13] Ugwuoke, I. C., 2011, Development and Design of Constant-Force Compression Spring Electrical Contacts, AU Journal of Technology, 14(4), 243-252.

[14] Ugwuoke, I. C., Abolarin, M. S., 2017, Non-Dimensionalized Parameter Development for Class 2B-lpl Compliant Constant-Force Compression Slider Mechanism, 2nd International Engineering Conference of the School of Engineering and Engineering Technology, Federal University of Technology, Minna, 17th-19th of October, 2017, 378-382.

[15] Ugwuoke, I. C., Abolarin, M. S., 2019, Design and Development of Class 2B-lpl Compliant Constant-Force Compression Slider Mechanism, International Journal of Engineering and Manufacturing, 9(3), 19-28.

[16] Weight, B. L., 2001, "Development and Design of Constant-Force Mechanisms", M.S. Thesis, Brigham Young University, Provo, Utah.